

Sensitivity Analysis of a Thermal Model of the Electron Beam Melting Process to Predict the Melt Pool Dimensions



Prepared for: Polytechnic University of Turin, Department of Management and Production
Engineering (DIGEP),

Prepared by: Farshid Khademi, Master of Mechanical Engineering

Thesis submitted to fulfill of the requirement for the degree of MSc. in Mechanical
engineering

Supervisors: Prof.Luca Iuliano, Dr.Manuela Galati

February 6, 2019

ACKNOWLEDGEMENT

I would first like to thank my thesis advisor Prof. Luca Iuliano and Dr. Manuela Galati of the Department of Management and Production Engineering at Polytechnic University of Turin. Their offices were always open whenever I ran into a trouble spot or had a question about my research. They always but steered me in the right the direction whenever I needed it.

Finally, I must express my very profound gratitude to my parents for providing me with unfailing support and continuous encouragement throughout my years of study and through the process of researching and writing this thesis. This accomplishment would not have been possible without them. Thank you.

Author

Farshid Khademi

ABSTRACT

In recent years, the scientific and industrial relevance of additive manufacturing has grown. In the metal area electron beam technology offers high power density as well as considerable scanning rates. Therefore, electron beam melting (EBM) seems to be suitable for processing a broad variety of alloys in an economic way. However despite of these improvement this technology has a long way to go and need to be developed in all aspect of industrial point of view.

Melt pool size and shape are key characteristics to control the process of EBM. Control of melt pool dimensions will greatly increase the ability to successfully build shapes, and may play an important role in controlling solidification microstructure.

In this thesis, we present an approach for obtaining melt pool dimensions through a thermal finite element simulation in which three aspects are developed and illustrated:

- Thermo-mechanical modeling of the growth process, based on Finite Elements (FE), which considers changes in the behavior of the material (powder to liquid to solid) through the finite element on melt pool ;
- Sensitivity analysis of the model to the physical characteristics of the material such as Porosity and Preheating Temperature. This is an important aspect allowing to focus on the most significant parameters to be determined experimentally with high reliability;
- Evaluation of the effects of different process parameters such as Beam Diameter on the process.

The article illustrates the theoretical thermal model and the detail of the strategy used in the FE analysis. The most influential characteristics of the material are highlighted and, finally, general criteria for choosing the optimal combination of process parameters are provided.

Contents

Introduction	5
Sensitivity Analysis	8
INTRODUCTION	8
SENSITIVITY TO MATERIAL PROPERTIES	9
SENSITIVITY TO PROCESS PARAMETERS	10
THERMAL BALANCE AND HEAT TRANSFER	11
MODEL OF THE EBM HEAT SOURCE	13
MATERIAL CHARACTERISTIC	15
FINITE ELEMENT MODEL	17
Process Analysis	19
PROBLEMS	21
CONTEXT CHARACTERIZATION	22
HYPOTHESES	23
INITIAL AND BOUNDARY CONDITIONS	24
SIMULATION PROCESS	25
RESULT ANALYSIS	32
Conclusion	41
PERSPECTIVE AND OBJECTIVES	41
PROJECT OUTLINE	44
Bibliography	45

INTRODUCTION

In recent years, the scientific and industrial relevance of additive manufacturing has grown. Electron beam-based additive manufacturing processes is being seriously considered for manufacturing and repair applications in various industries. The electron beam technology (EBM) offers high power density as well as considerable scanning rates. Therefore, it seems to be suitable for processing a broad variety of alloys in an economic way. At the low power range, Laser Engineered Net Shaping, has been used to create complex prototypes, tooling, and small-lot production items with the ability to manufacture shapes based on geometry from CAD solid models (1). Using a similar approach, Electron Beam Manufacturing (EBM) processes are being considered for manufacturing aerospace components and etc. Like their laser-based counterparts, in EBM, parts or features are built up layer-by-layer with the beam serving as a moving heat source (1). Electron beam-based processes offer more advantages over laser-based processes, including more efficient energy transfer to the substrate, transfer efficiencies that are not a function of the reflectivity of the substrate and the ability to rapidly move the electron beam across the surface or within the melt pool to locally tailor surface temperature fields.

By means of mathematical–physical modeling, process stability of the melting step is being increased. Moreover, by solving a detailed thermal model using the finite element method (FEM), substantial knowledge of adequate parameter settings in dependence of the utilized material is developed.

The use of an electron beam offers extensive potentials such as higher build rates due to increased penetration depths and elevated scanning velocities. For example, by using several beam spots, an enormous reduction of the time required for the powder solidification can be realized. However, EBM parts still exhibit comparatively coarse surfaces. The basic procedural principles of EBM is almost identical: a focused electron beam is deflected in order to solidify a metal powder selectively, processing a layer of a thickness ranging from 20 to 100 μm (2). Differences can be observed in the processable materials and within the individual process and scanning strategies.

In 1997, patents led to the founding of the Swedish company ARCAM AB, that distributes the two systems EBM S12 and A2. Taminger et al.(3) and Dave´ (4) suggested the use of wire feed systems to produce parts by means of an electron beam. At the “iwb Application

Center Augsburg”, experimental equipment was developed in order to generate the required geometry from powder materials.

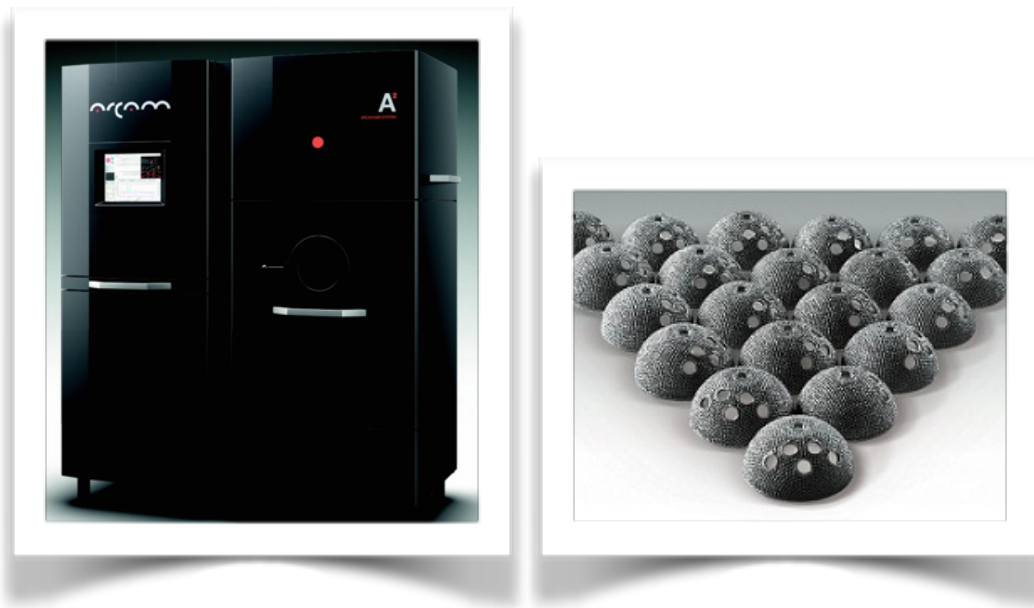


Fig.1. EBM machine produced by ARCAM, A2 model (refer to ARCAM website)

EBM machine is maintained at high vacuum and elevated temperatures (650-700°C) to avoid oxidation and reduce internal stresses. The build process conditions in EBM have the ability to fabricate near net shaped and fully dense Ti-6Al-4V parts with microstructures of fine needle-like phase separated a by phase. The EBM parts have found applications in medical implants (5) to aerospace parts. Numerous research has been carried out in studying the microstructures obtained in EBM Ti-6Al-4V (6) and its variation as a function of process parameters (7), build height (8), part thickness (9) and for complex geometric shapes (10).

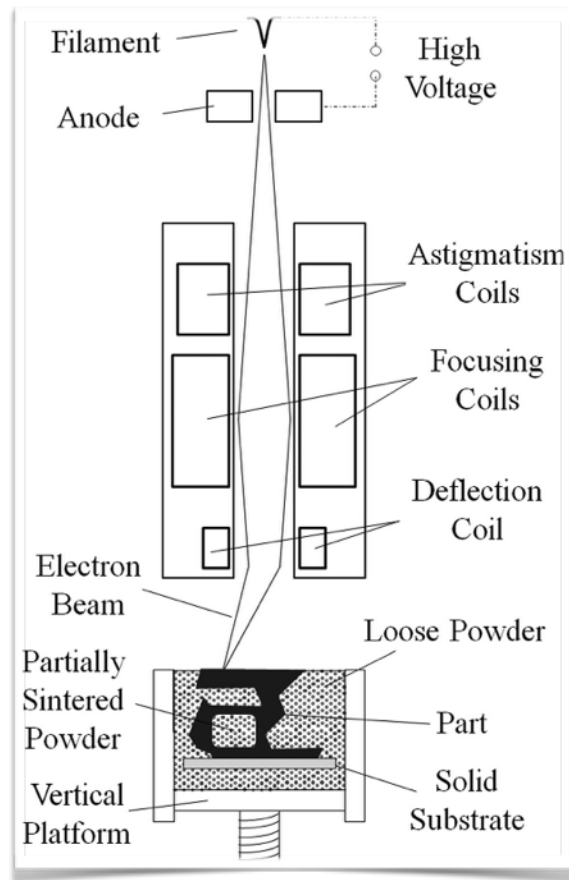


Fig.2. Schematic of the components of EBM setup (11)

The need of post processing leads to decreased manufacturing speeds and higher costs. Therefore as EBM offers near net shape production, even for complex geometries, with little material waste which enables large weight saving possibilities, seems to be a more efficient method although it still needs to be developed(12).

SENSITIVITY ANALYSIS

1. Introduction

Sensitivity analysis is focused on the effect of changing in some essential parameter on the output, product or result of a process. The other name of sensitivity analysis is “what if analysis”, so in this thesis we show how the change of some parameters like beam diameter, porosity, etc, effect the final process and the final product through simulations.

Uncertainty in the estimation and use of parameters is common in system modeling. In many situations, the accurate measurement of values, represented by parameters in the model, is difficult and sometimes impossible.

Sensitivity analysis offers a means to quantify and rectify this problem. The goal of sensitivity analysis is to mathematically quantify the behavior of the model to small changes in its parameters. A small change in a parameter resulting in a large change in the output of the model shows a high influence (sensitivity) of the parameter on the model behavior. In this case, the estimation of the parameter needs to be as accurate as possible.

Sensitivity analysis allows for the determination of the accuracy of the parameters that make the model useful, i.e., behaves in accordance with “real world” expectations. Besides detecting critical parameters in the model, sensitivity analysis also provides optimistic and pessimistic estimation of the project outcomes based on combined changes in the input parameters (13).

There have been a number of research studies reported about the effects of AM process parameters on the process performance and outcome. Experiments are often conducted to validate predicted temperature distribution (temperature [K]) and melt pool size (length, width, and depth [μm]), however, most of these researches have been focused on laser based additive manufacturing sensitivity. to mention a few:

In (14) Jerzy Kozak and Tomasz Zakrzewski have performed sensitivity analysis for one-dimensional (1D) thermal model determined influence of changes in laser beam parameters (power, spot diameter, exposition time) and changes in powder layer properties on dimensions of single track of molten material. Consequently to quantify how changes in the design parameters (design variables) affect the value of response to increase the accuracy of the final part dimensions. The design parameters is been categorized as follow: (14)

- Geometrical process parameters (e.g. dimensions such as laser spot diameter)
- Powder parameters

- Fabrication design parameters (e.g. power density, pulse time on, pulse time off, laser scan speed).

in which sensitivity has been described with sufficient accuracy (as it is assumed) the relation between value of response R and values of design parameters:

$$R = R(p_i^g, p_j^m, p_k^f) = R(p_l)$$

Moreover, In (15) A physics-based analytical 2D model is proposed in order to predict the temperature profile during metal additive manufacturing (AM) processes, by considering the effects of temperature history in each layer, temperature-sensitivity of material properties and latent heat. In order to illustrate the importance of considering the temperature dependent material properties, a sensitivity analysis is conducted to compare the predicted surface temperature with and without considering the property's temperature-sensitivity. The proposed analytical model is used to predict the melt pool size. A comparison between the model and experimental results are conducted. The analytical model of the temperature is based on the moving heat source assumption.

Regarding the sensitivity analysis in this model, The effect of different process parameters such as laser power and scanning speed and material properties such as thermal conductivity on the temperature profile, surface temperature, and also peak temperature are investigated and the relations between them are established. Also these process parameter has been used to predict the melt pool geometry. The predicted temperature from the analytical model are compared with the experimental values and FEM results.(15)

On the other hand, In this thesis work some other characteristics of material properties and process parameter have been focused on to obtain accurate effects on the melt pool size in EBM. which will be discussed as follow:

2. Sensitivity to material properties

Since we are working on a numerically-based solution, the results will also be sensitive to several finite element-related parameters: length and width of the workpiece, number of elements in the mesh, and time (16). This thesis focused on the effect of density, preheating temperature as material properties. Table (13) shows the comparison of simulation results for several FE model numerical parameters.

The melt pool geometry is obtained by noting the nodes where the temperature is above the liquidus temperature. The following table (Table 1) shows the value used in the base simulation. The simulation was run for 3 different densities and each density has been corresponded with 3 different preheating temperature and for each preheating temperature 3 different beam diameter has been considered. By modifying a single parameter its effect can be analyzed individually and independently.

Other physical properties of the bulk and powder material parameters including latent heat of fusion, specific heat, and bulk thermal conductivity has been model through FEM and has been constant for simulations.

	1	2	3
Density [kg/mm³]	2.67 E-06	2.28 E-06	1.89 E-06
Per-heating Temp [°K]	773	973	1173
Latent Heat [kJ/kg]	273	273	273
Liquidus Temp [°K]	1699	1699	1699
Solidus Temp [°K]	1658	1658	1658
Porosity	0.32	0.42	0.52

Table(1): Sensitivity to material properties

3. Sensitivity to process parameters

The influence of process parameter variation on the predicted temperature profile (peak temperature and time above liquidus temperature) and melt pool geometry (length, width and Depth) was investigated for EBM. The following table (Table2) shows the value used in the base simulation for EBM process parameters, as well as the resulting value for each parameter. Each simulation was run by modifying a single parameter, density, and leaving all other process parameter values constant. An identical sensitivity analysis is performed, this time with EBM process parameters instead of material properties. The evolution of temperature as a function of time at a fixed location is chosen to show the effect of 3 different spot-size diameter of the electron beam. Electron beam power and scanning speed has been considered as constant parameters for each simulation.

4. Thermal balance and heat transfer

In order to model the EBM process, many physical aspects must be taken into account. During the creation of a component electron beam scans a thin layer of metal powder and heats up a small cell until the melting temperature is reached; afterwards the cell cools down again as the melt pool moves away. In this process, the material undergoes many state transformations (powder to liquid to solid), density change, material structure changes. Moreover, the same cell will be cyclically heated up and cooled down as the electron beam impinges neighboring regions of the same layer or the corresponding region of the next layer.

A model of the process must consider all these aspects which depend on temperature history; the main problem to be addressed is therefore the mathematical formulation of the thermal process. A balance of heat input and heat output in a single cell must be established. During the EBM process, the heat input is represented by the electron beam energy absorbed by the layer surface and the heat outputs are represented by heat losses from the cell due to conduction, radiation and convection,(17). The balance between input and output heats up the cell and supplies the latent heat to melt the powder (18).

the formation of the melt pool is closely correlated to the wet-ability of the material, whereas the Marangoni convection flows affect the dynamics of the melt pool. In order to simplify the analysis, the uncoupled models only consider the main phenomena that can cause the heat transfer (19).

To govern the equation of the thermal balance and calculation of the temperature distribution, energy conservation has been considered in an uncoupled heat transfer analysis (19):

$$-\nabla \cdot \mathbf{q} = \rho \frac{De}{Dt}$$

Where \mathbf{q} is the heat flux vector, $\rho = \rho(\mathbf{T})$ is the density and \mathbf{De}/\mathbf{Dt} is the material derivate of the thermal energy density. The thermal energy density e can be written as:

$$e = cT + \Delta h$$

where c is the specific heat, $\mathbf{T}(x_1, x_2, x_3, t)$ is the temperature, which is a function of both space and time \mathbf{t} , and Δh is the latent enthalpy, which is defined as: (19)

$$\Delta h = \begin{cases} L & T \geq T_l \\ \frac{T - T_s}{T_l - T_s} L & T_s < T < T_l \\ 0 & T \leq T_s \end{cases}$$

where T_s and T_l are the solidus and liquidus temperatures, respectively, and L is the latent heat of fusion. The surface heat flux vector \mathbf{q} is described by Fourier's law as:

$$\mathbf{q} = -\lambda \nabla T$$

where $\lambda = \lambda(T)$ is the thermal conductivity. The heat transfer problem, corresponding to the initial and boundary conditions, is solved. The initial and boundary conditions are expressed as:

$$\begin{aligned} T(x_1, x_2, x_3, 0) &= T_{preheat} \text{ with } (x_1, x_2, x_3) \in D \\ T(x_1, x_2, x_3, 0) &= T_r \text{ with } (x_1, x_2, x_3) \notin D \\ T(x_1, x_2, x_3, \infty) &= T_r \text{ with } (x_1, x_2, x_3) \notin D \\ -\lambda \frac{\partial T}{\partial n} \Big|_{beam} &= q - q_{rad} \\ -\lambda \frac{\partial T}{\partial n} \Big|_{topsurface} &= -q_{rad} \end{aligned}$$

where D is the union between the substrate and the layer domains. The heat flux \mathbf{q} represents the energy source. $T_{preheat}$ and T_r are the preheating temperature and the build chamber temperature, respectively.

The heat loss, q_{rad} , due to radiation can be expressed as:

$$q_{rad} = \varepsilon \sigma (T^4 - T_r^4)$$

where $\varepsilon = \varepsilon(T)$ is the emissivity and σ is the Stefan-Boltzmann constant, whose value is $5.67 \cdot 10^{-8} \text{ Wm}^{-2} \text{ K}^{-4}$.

	1	2	3
Beam Diameter [mm]	0.2	0.3	0.4
Beam Power [kW]	50	50	50
Scan Speed [mm/s]	2.3	2.3	2.3

Table(2): Sensitivity to process parameters

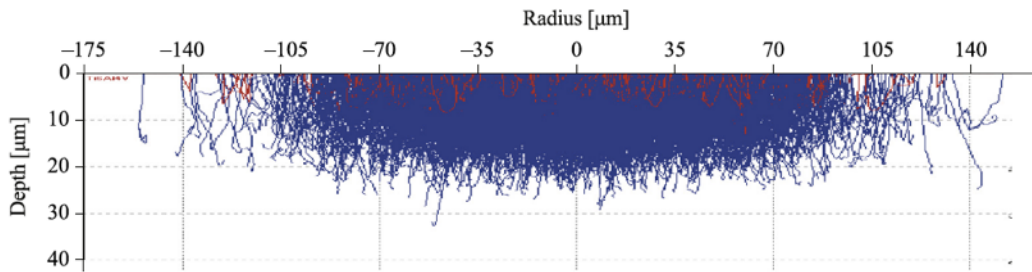


Fig. 3. Electron trajectories in a cross-section of a Ti6Al4V sample. The electron trajectory simulation has been performed with the CASINO software. The red lines refer to back-scattered electron trajectories, while the blue lines refer to the paths of non-back-scattered electrons. An acceleration voltage of 60 kV and a beam diameter of 0.272 mm have been used.(20)

5. Model of the EBM heat source

For the modeling of the heat source, the new type of modeling introduced by Galati, Iuliano et al. 2017 (20) has been used. In this model, the impact of the electron beam on the preheated powder bed was studied by means of simulation with the Monte Carlo method (20). This method estimates the trajectories of the electrons within a sample, taking into account the mean free paths of the electron and the probability of interaction of the phenomena that occur during collision (20). The factors that play key roles are the material density, the alloy elements and their atomic number, the energy or accelerating voltage of the beam, and the focus beam diameter. The simulations were run for several materials and several focus beam diameters that are generally used in the EBM process, assuming the beam had a perpendicular impact with the top surface.

An Abaqus DFLUX user subroutine has been used to apply the heat flux to the top surface of the layer (Fig 4). The location of this flux changes with time due to the movement of the beam. The DFLUX subroutine is used to define the flux distribution as a function of the position and time. The user subroutine DFLUX is called at the beginning of each time increment and at each flux integration point. It then reads the simulation time and calculates the current position of the center of the electron beam. The user code includes the motion law of the beam (scanning mode), the analytical formulation for the energy source and the

equation to select the surface where the heat flux is applied. For example, following equation simulates the movement of the beam spot along the x_1 axis:

$$(x_1 - x_{10} - \dot{x}_1 t)^2 + (x_2 - x_{20})^2 \leq \left(\frac{D}{2}\right)^2$$

where \dot{x}_1 is the beam scan speed, expressed in $mm s^{-1}$, D is the beam diameter and x_{10} and x_{20} are the coordinates of the starting point of the beam center along the x_1 and x_2 axis, respectively, and the millimeter is used as the unit of length.

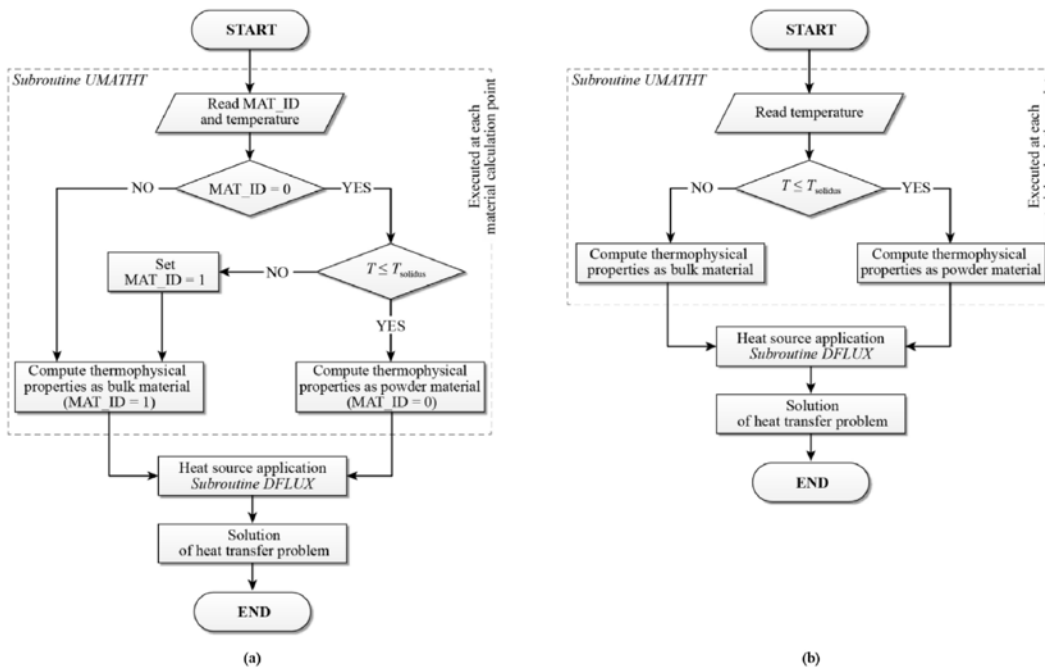


Fig.4. (a) the DFLUX and UMATHT subroutines with material change procedure, (b) the DFLUX and UMATHT subroutines without material change procedure

6. Material characteristic

Material microstructure plays an important role in EBM process control, due to mechanical property requirements in finished parts. Finite element simulations have been used to observe cooling rates and thermal gradients.

A study of process variable (beam power and velocity) effects shows that microstructure can vary significantly along the depth of the deposit. It was shown experimentally in (21) that melt pool size and cooling rate significantly depend on the travel velocity and laser power.

Temperature variety involved in the EBM process, makes the thermo-physical properties as functions of the temperature. However, the thermal behavior of the powder and of the bulk material is significantly different. Consequently, when the temperature is higher than the melting point, the thermo-physical properties of the powder are the ones that correspond to the properties of the liquid metal. After melting and during cooling, the thermo-physical properties become those of the bulk. The melting phase of the powders causes the material state change from powder properties to the bulk properties. Thus, the thermal behavior is a function of the temperature and of the material state. The temperature dependent values of the bulk material have been extracted from technical databases (20). The properties of the corresponding powder material have been calculated from the respective bulk material by applying the specific models described in (20) in which:

$$\rho_{powder} = (1 - \varphi) \rho_{bulk}$$

where ρ_{powder} is the powder density and ρ_{bulk} is the bulk density. In this model, the powder density is assumed continuum, therefore the material properties has been defined of any particular coordinate.

Thermal conductivity and emissivity has been modeled as thermal properties (20). Thus, UMATHT is used to compute the specific heat, the thermal conductivity, and the material state change and the phase change. The required inputs are listed below (20):

- Thermal conductivity of the bulk material (λ_{bulk}) as a function of the temperature
- Specific heat (c) as a function of the temperature
- Latent heat
- Solidus temperature

- Liquidus Temperature
- Powder porosity
- Neck ratio
- Particle size
- Stefan-Boltzmann constant

In (22) The EBM build used is Ti-6Al-4V ELI gas atomized powder provided by Arcam. the ELI variant of Ti-6Al-4V contains reduced levels of oxygen, nitrogen, carbon, and iron. The powder used was a mixture of 50% new powder and 50% powder reused from a previous build, with a particle diameter ranging from 45 to 150 μm , Fig. 5

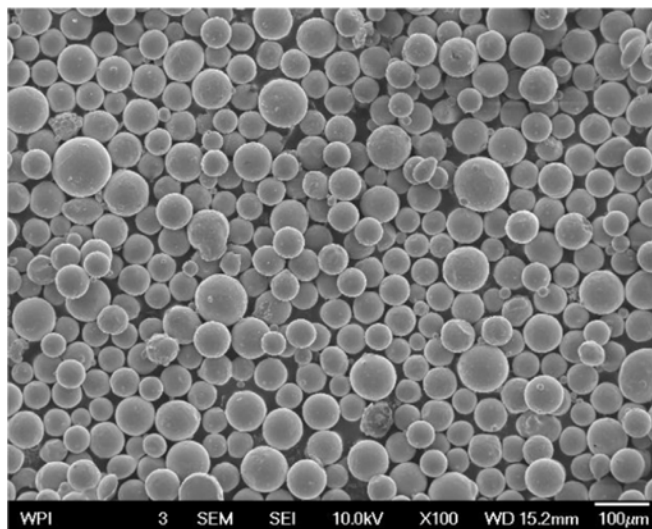


Fig.5. Ti-6Al-4V ELI powder particles used to fabricate the EBM samples (22)

7. Finite element model

Numerical-based modeling and simulation methods, are a useful complement for understanding the thermal history in metal-based AM processes. The Finite Element (FE) method has been shown to be a versatile and accurate numerical method for solving engineering problems (e.g., heat transfer, solid mechanics, fluid dynamics) (23), even for complex geometries and irregular meshes (24). Over the past two decades, a significant number of FE models have been developed to simulate various aspects of AM processes, with particular emphasis on investigating the thermal history, melt pool geometry, and residual stresses (11);(25). Most existing validation efforts of FE models, however, have either focused on comparing the predicted melt pool size and geometry with experimental measurements, or the thermal history in the case of single-track deposits (26);(25).

The present paper is intended to evaluate the sensibility of the model with respect to uncertainties on the real value of the main physical proprieties of the material in order to understand where to concentrate the experimental characterization activity. The model also allows to choose the most promising combination of technological parameters (scan speed, EBM power, path overlapping).

The work is based on FE modeling of a thin stack of layers realized with EBM technique, the material considered is Titanium (Ti6AlV), a material often used in industrial applications; the bulk characteristics of (Titanium Ti6AlV) can be found in (27).

The complexity of the EBM process because of the factors such as high scan speed, rapid phase change, non homogeneous temperature distribution, makes the necessity simplification in the FEM model, so only the main phenomena that cause the heat transfer have been considered in the model, such as conduction between the powder particles and between the powder bed and the bulk substrate, as well as irradiation from the powder bed to the chamber, which have been discussed in section 2.

The more relevant simplified hypotheses adopted in the work are:

- The thermal characteristics are assumed to be linearly dependent from temperature,
- The powder characteristics are assumed to be linearly dependent from porosity,
- Absorbance is assumed constant for powder and bulk material,
- Assumption of perfect wetting
- Negligible capillarity forces and evaporation

A single thick layer is modeled on the top of the substrate as unsintered powder. The mesh consists of 8-node linear heat transfer DC3D bricks. A specific finer mesh was used within a portion of the powder layer of where and in the proximity the heat flux was applied. This mesh strategy was used to obtain detailed results on the inside of the powder layer close to the incident electron beam. However, the size of the mesh elements was also chosen to avoid long running times and to ensure the absence of spurious oscillations in the solution, caused by a numerical relationship between the minimum usable time increment, the element size and the thermo physical properties. The electron beam flux moves along the x1 axis to simulate a single track.

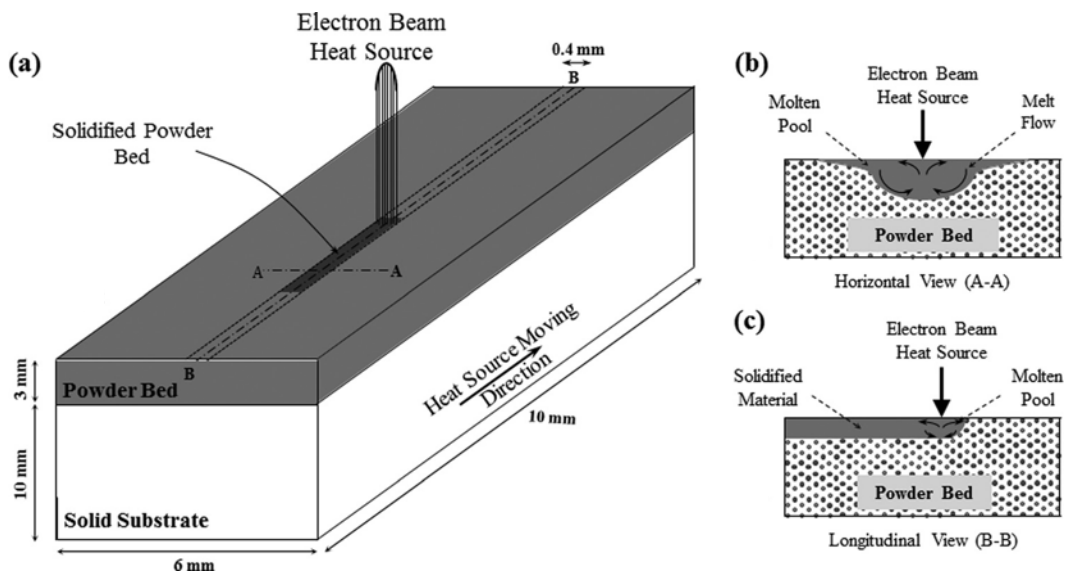


Fig.6. The geometry of the part; (a) the part overview, (b) horizontal view of the part cross-section, and (c) longitudinal view of the part cross-section (11)

PROCESS ANALYSIS

Electron Beam Melting (EBM) process is based on metal powder melting through high energy beam. EBM is able to produce complex parts made of excellent quality material. The EBM process can be used to work with many different material classes, such as stainless steel (17-4), tool steel (H13), Ni-based super alloys (625 and 718), Co-based superalloys (Stellite 21), low-expansion alloys(Invar), hard metals (NiWC), inter-metallic compounds, aluminum, copper, beryllium and niobium [26]. Nevertheless, the use of this technology is at present focused on Titanium Ti6AlV.



Despite having extensive advantages over conventional manufacturing technologies, EBM still exhibits several process deficiencies. After finding the deficiencies of the process of EBM, improvement should be done through the simulation. For the evolution of simulation model we need to understand the important parameters involved in the Process of EMB which have been discussed in pervious section (Sensitivity analysis) and try to improve them by different technics.

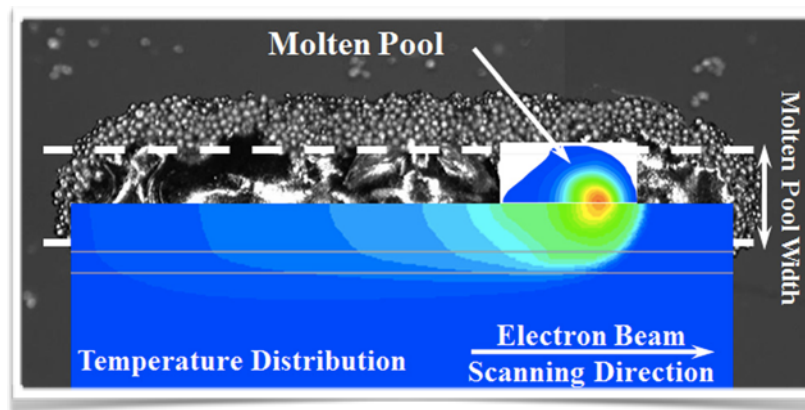


Fig.7. EBM scan direction and temperature distribution regarding melt pool dimensions (11)

Ti-6Al-4V and Alloy 718 are two alloys that are widely used in aerospace applications. Ti-6Al-4V amounts to 80% of the total titanium alloys volume used within the aerospace sector whereas Alloy 718 is the most used Ni-based alloy within e.g. GE aircraft engines being an important alloy for rotating parts and at temperatures exceeding titanium's limit. AM of titanium has many advantages compared to conventional manufacturing because titanium is regarded as an expensive material compared to e.g. steel. The high production price for conventional manufacturing is partly due to that up to 80% of the titanium is machined away and due to titanium's high affinity to oxygen making it a complicated metal to work with. If titanium is exposed to oxygen at high temperatures an oxide layer called α -case is formed, which reduces the mechanical properties. The problem with titanium's affinity to oxygen is no issue when using EBM because the manufacturing takes place in vacuum. One of the main reasons for using titanium is that this metal has low density while having good mechanical properties giving it a high specific strength. Titanium is furthermore a good choice for use in harsh environments as it has good corrosion resistance in most environments. In EBM, along with other AM processes (28).

1. Problems

The process simulation and analysis of EBM technology has been contained various obstacles.

To mention a few:

The during the simulation process one of the problems we have been faced was the Beam diameter, which at the first attempt we tried to use the real dimension which is more feasible to be validate experimentally, but in the calculation it was not possible to fix the real dimensions according to the nodes we have been considered based on the FE model, therefore the dimensions recalculated based on nodes arrangement.

As it has been discussed in the pervious sections, Here we tried to define a coefficient to correlate the bulk density and the powder density somehow it can be used instead of large number of parameters in the sensitivity analysis. which decreases the simulation time significantly. Theoretically the model has been discussed in (20). but the problem lies into how we can measure this coefficient in practice for the experiment.

In this regard, an Idea has been proceed to calculate this coefficient by considering firstly the density of a fully processed part (bulk density) and secondly the density of the part while it has not been fully processed, consequently the difference will provide us the powder density for the same part, although this method seems to be very challenging to obtain accurate amount of the density, but it could be useful of the moment.

$$\rho_{powder} = (1 - \varphi) \rho_{bulk}$$

2. Context Characterization

The powders used in the EBM process are usually produced by gas atomization, and the obtained particle shape is spherical. The main parameters that characterize the powder particles are size distribution and relative density. The density of the powder bed is usually assumed to be equal to 68% of the corresponding solid density. Hence, it can be assumed that the powder can be approximated as a packed bed of equal spheres with a mean radius, while the relative packing density corresponds to the BCC atomic packing factor.

On the whole, the effect of porosity ϕ_S here has been considered at 3 different amount equal to 0.32– 0.42– 0.52 respectively and preheating effect which before the melting phase sinters the powder particles that form the circular necks is been investigated for each porosity separately.

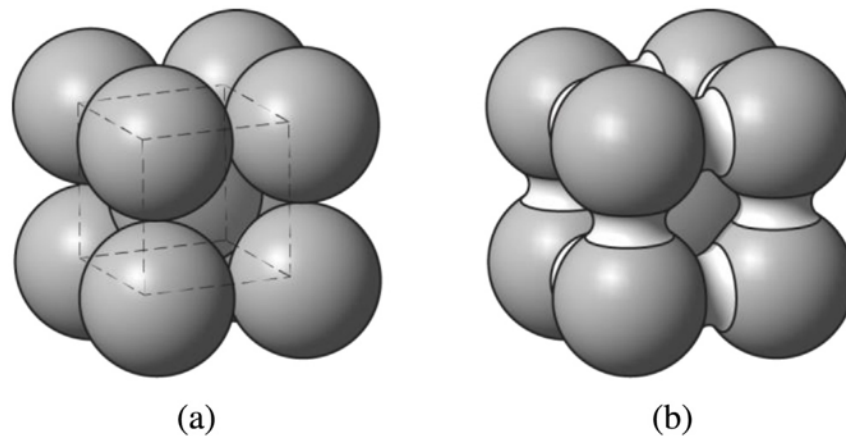


Fig. 8. (a) The model of a powder (BCC structure) before the preheating phase, (b) the model after the preheating phase. (20)

3. Hypotheses

Due to temperature dependent material properties and a moving heat source, an analytical solution of the thermal process model is considerably demanding. Therefore, the mathematical – physical model is being transferred into a simulation software based on the finite-element-method (FEM) and thus, melt pool characteristic as a function of various input parameters has been predicted. After the interpretation of the results, the validation by means of temperature measurement is being conducted in order to calibrate the existing simulation model. Consequently, know-how is being generated from the simulation experiments leading to the definition of a process window for the fabrication of dense EBM parts. Due to the early development phase of this technology, further quality characteristics (e.g. surface roughness) are not considered.

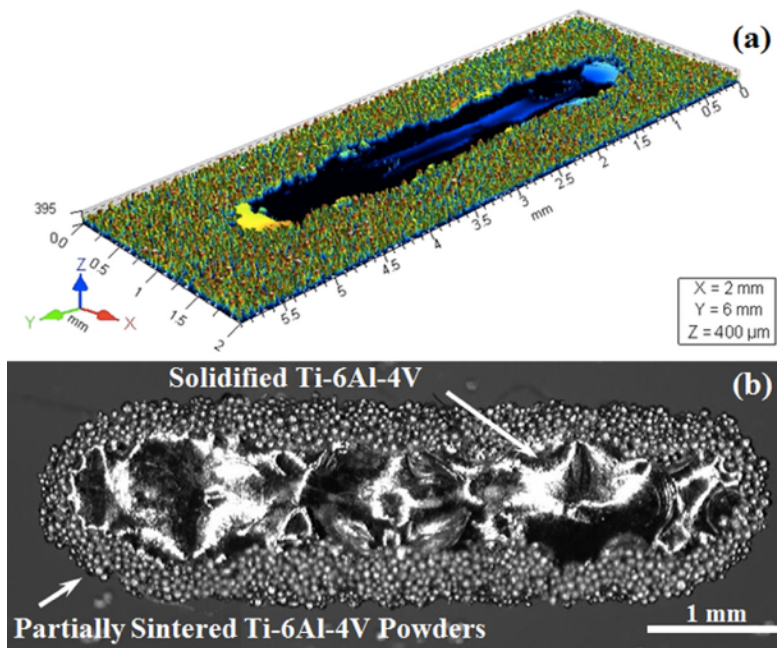


Fig. 9 Electron beam melted Ti-6Al-4V trace, (a) The 3D image of the electron beam trace provided by profile meter and (b) The image of the electron beam trace provided by optical microscope (11)

4. Initial and boundary conditions

The plate is the upper and lower surfaces as shown in Fig. 10. Both convection and radiation conditions are considered in all external surfaces. The power absorption efficiency, η is 0.13. The ambient temperature is 25 °C. For all the simulations, The initial temperature of the entire build was set and expressed as:

$$T(x, y, z, t)$$

The temperature on the boundary surfaces, except the top surface, was maintained at the ambient temperature during the simulation. Both natural convection and radiation were applied on the top surface as the boundary conditions.

These conditions can be expressed as:

$$q_{\text{convection}} = h (T_{\text{amb}} - T)$$

$$q_{\text{radiation}} = \varepsilon \sigma_B (T_{\text{amb}}^4 - T^4)$$

where h , T_{amb} , T , ε , and σ_B are the convective heat transfer coefficient, ambient temperature, current temperature, surface emissivity, and Stefan–Boltzmann constant, respectively.

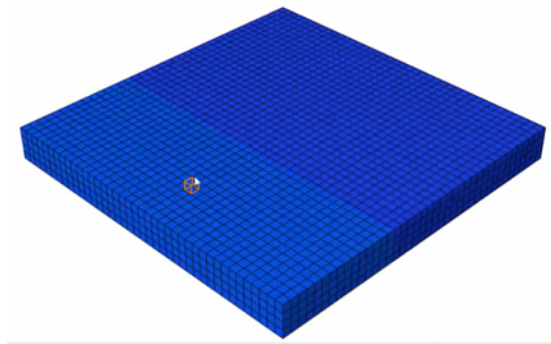


Fig.10 Plate model in ABAQUS

5. Simulation Process

By considering all the matters in previous sections, the simulation has been run 27 times to evaluate all the consequences of each factors. The effect of the factors “Preheating temperature”, “Beam diameter” and “Porosity” on melt-pool characteristic has been investigated separately in each simulation run.

A fixed time step 0.00431 s has been consider in order to record the result and carry out accurate comparison. The measuring of melt-pool dimension has been scaled through out the photos form ABAQUS model.

Here in below the simulation process and the recorded result is been presented:

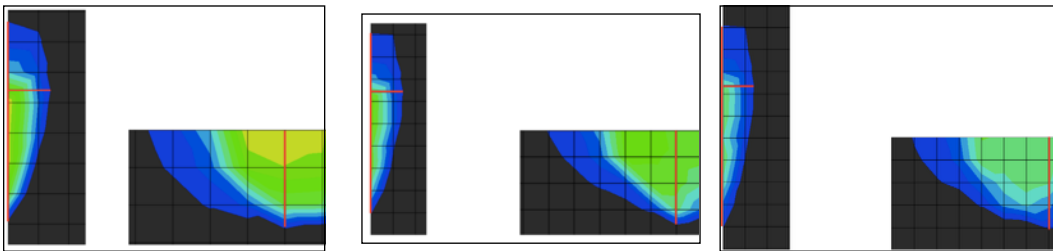


Fig.11: ABAQUS photo of 3 Beam diameters effect on melt-pool dimensions

(T preheating: 773 °k and porosity: 0.32)

Simulation Nr.	Beam Di. [mm]	Width [mm]	Length [mm]	Depth [mm]	Melt-pool max T[°K]
1	0.2	0.2554	0.3292	0.0707	3228.15
2	0.3	0.3526	0.4106	0.0734	2895.95
3	0.4	0.4166	0.4595	0.0702	2641.75

Table (3): Effect of 3 Beam diameters on melt-pool characteristics at Porosity 0.32 and preheating temperature 773 °k

In the first 3 simulation run, the porosity at 0.32 and preheating temperature at 773 °k have been kept constant and the result has been recorded as above in Table (3), and Fig.11

In the second 3 simulation run, we kept the porosity at 0.32 and increase the preheating temperature to 973°k, and the result is recorded as below:

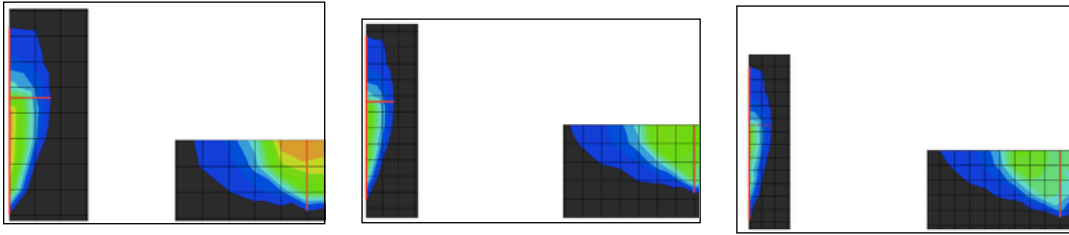


Fig.12: ABAQUS photo of 3 Beam diameters effect on melt-pool dimensions

(T preheating: 973°k and porosity: 0.32)

Simulation Nr.	Beam Di. [mm]	Width [mm]	Length [mm]	Depth [mm]	Melt-pool max T[°K]
4	0.2	0.2698	0.3733	0.0833	3374.45
5	0.3	0.365	0.5121	0.0878	3046.99
6	0.4	0.4686	0.6178	0.0892	2799.48

Table (4): Effect of 3 Beam diameters on melt-pool characteristics at Porosity 0.32 and preheating temperature 973 °k

At this point, we raised the preheating temperature to 1173°k at the same porosity and recored the effects at the same time step.

Results for the 3rd three runs of simulation have been recorded in Fig.13 and Table (5):

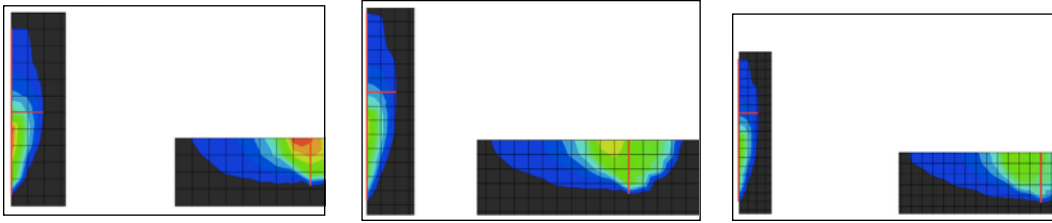


Fig.13: ABAQUS photo of 3 Beam diameters effect on melt-pool dimensions

(T preheating: 1173°k and porosity: 0.32)

Simulation Nr.	Beam Di.[mm]	Width [mm]	Length [mm]	Depth [mm]	Melt-pool max T[°K]
7	0.2	0.2826	0.5255	0.1011	3504.93
8	0.3	0.375	0.6882	0.1073	3213.14
9	0.4	0.492	0.8675	0.115	2990.48

Table (5): Effect of 3 Beam diameters on melt-pool characteristics at Porosity 0.32 and preheating temperature 1173 °k

The effect of beam diameter and preheating temperature is recorded for porosity 0.32, at this point, by increasing the powder porosity (reducing the powder density), we run the simulation with same beam diameter and preheating temperature as pervious 9 simulation run. Here in below, the result is presented:

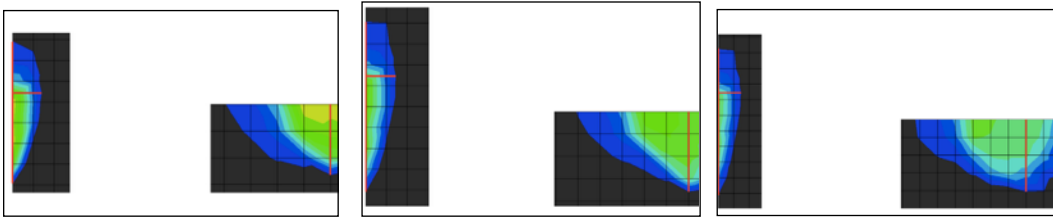


Fig.14: ABAQUS photo of 3 Beam diameters effect on melt-pool dimensions
(T preheating: 773°k and porosity: 0.42)

Simulation Nr.	Beam Di. [mm]	Width [mm]	Length [mm]	Depth [mm]	Melt-pool max T[°K]
10	0.2	0.276	0.3401	0.0705	3238.91
11	0.3	0.3568	0.4141	0.0735	2903.76
12	0.4	0.418	0.4907	0.0763	2690.02

Table (6): Effect of 3 Beam diameters on melt-pool characteristics at Porosity 0.42 and preheating temperature 773 °k

By increasing the Preheating temperature to 973°k, we have:

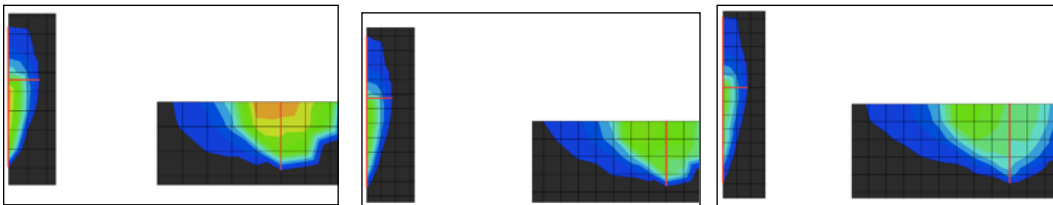


Fig.15: ABAQUS photo of 3 Beam diameters effect on melt-pool dimensions
(T preheating: 973°k and porosity: 0.42)

Simulation Nr.	Beam Di. [mm]	Width [mm]	Length [mm]	Depth [mm]	Melt-pool max T [°K]
13	0.2	0.2838	0.3735	0.082	3376.73
14	0.3	0.3764	0.5307	0.0897	3064.78
15	0.4	0.4638	0.6277	0.093	2839.04

Table (7): Effect of 3 Beam diameters on melt-pool characteristics at Porosity 0.42 and preheating temperature 973 °k

As for preheating temperature 1173°k with 0.42 porosity we have:

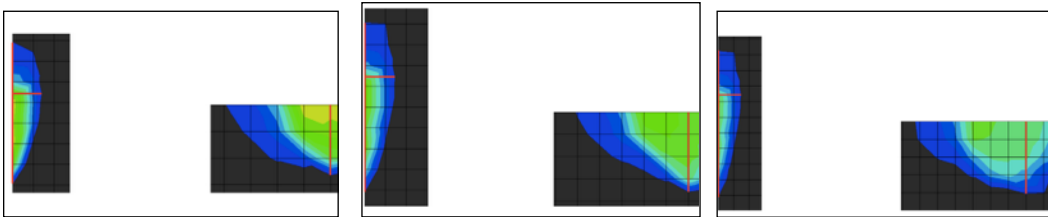


Fig.16: ABAQUS photo of 3 Beam diameters effect on melt-pool dimensions
(T preheating: 1173°k and porosity: 0.42)

Simulation Nr.	Beam Di. [mm]	Width [mm]	Length [mm]	Depth [mm]	Melt-pool max T [°K]
16	0.2	0.2918	0.5176	0.1014	3510.61
17	0.3	0.4064	0.6842	0.1071	3219.32
18	0.4	0.4758	0.8979	0.1208	3024.21

Table (8): Effect of 3 Beam diameters on melt-pool characteristics at Porosity 0.42 and preheating temperature 1173 °k

Now by increasing the powder porosity and run the simulation another 9 times we can evaluate accurately the effect of each parameter in the new condition:

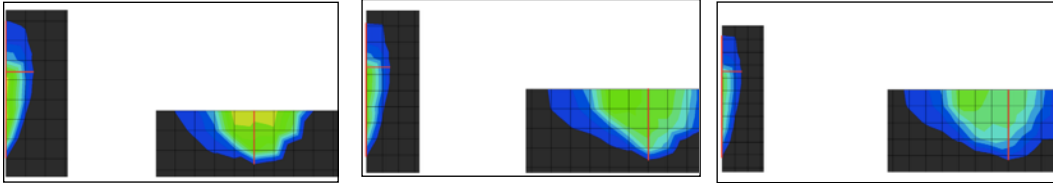


Fig.17: ABAQUS photo of 3 Beam diameters effect on melt-pool dimensions

(T preheating: 773°k and porosity: 0.52)

Simulation Nr.	Beam Di. [mm]	Width [mm]	Length [mm]	Depth [mm]	Melt-pool max T[°K]
19	0.2	0.2752	0.3611	0.073	3231.09
20	0.3	0.3592	0.4114	0.075	2922.79
21	0.4	0.436	0.4916	0.0819	2714.31

Table (9): Effect of 3 Beam diameters on melt-pool characteristics at Porosity 0.52 and preheating temperature 773 °k

And, as for higher preheating temperature 973°k we have:

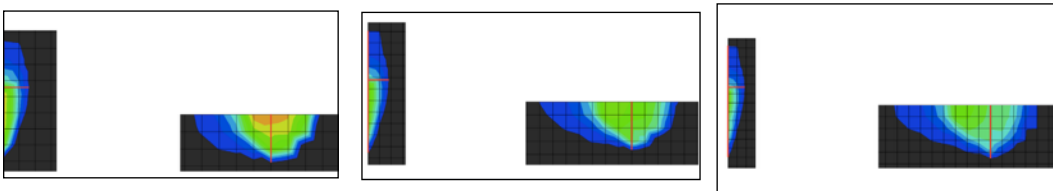


Fig.18: ABAQUS photo of 3 Beam diameters effect on melt-pool dimensions

(T preheating: 973°k and porosity: 0.52)

Simulation Nr.	Beam Di. [mm]	Width [mm]	Length [mm]	Depth [mm]	Melt-pool max T[°K]
22	0.2	0.2922	0.367	0.082	3352.38
23	0.3	0.3804	0.5472	0.093	3074.71
24	0.4	0.4686	0.6562	0.0979	2856.52

Table (10): Effect of 3 Beam diameters on melt-pool characteristics at Porosity 0.52 and preheating temperature 973 °k

And finally, the last three simulations have been considering the preheating temperature 1173°k for porosity 0.52 as below:

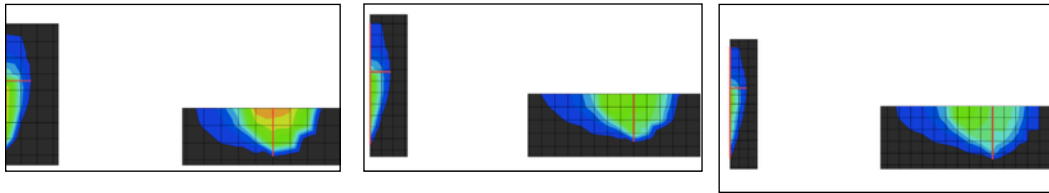


Fig.19: ABAQUS photo of 3 Beam diameters effect on melt-pool dimensions

(T preheating: 1173°k and porosity: 0.52)

Simulation Nr.	Beam Di. [mm]	Width [mm]	Length [mm]	Depth [mm]	Melt-pool max T[°K]
25	0.2	0.288	0.5236	0.1	3486.27
26	0.3	0.409	0.716	0.11	3221.04
27	0.4	0.5082	0.9409	0.125	3033.87

Table (11): Effect of 3 Beam diameters on melt-pool characteristics at Porosity 0.52 and preheating temperature 1173 °k

6. Result Analysis

In order to understand better the recorded results which have been presented in pervious section, data analysis and comparisons need to be done. In this section we try to point out the mean features of each parameter by using charts and diagrams:

In the first step, lets have a general look of the simulation results:

As far as melt-pool dimensions is concerned:

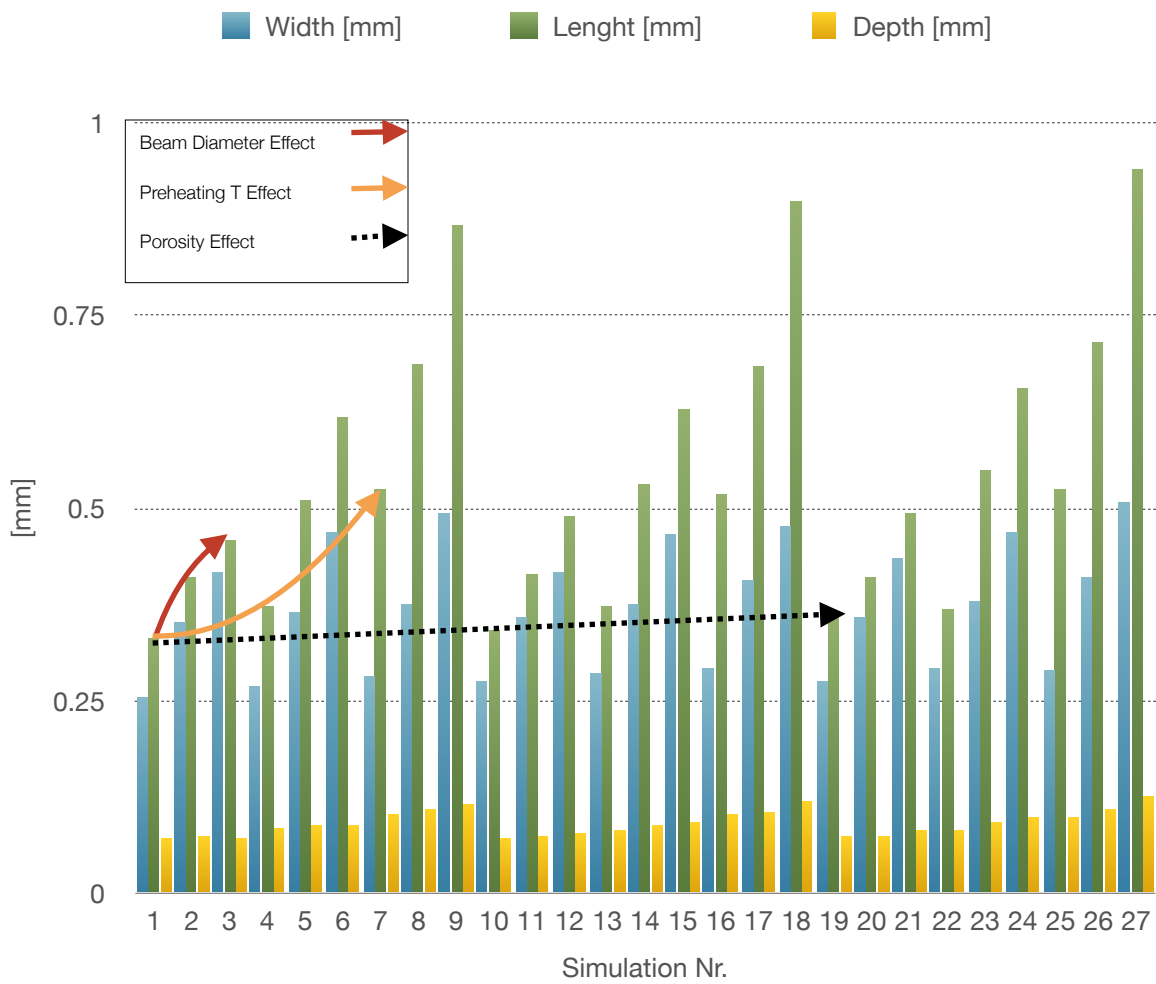


Fig.20: Melt-pool dimensions sensitivity to porosity, preheating temperature and beam diameter

In Fig.20, the effect of all the factors which have been focused on in this thesis work is presented. As it can be seen, in general point of view, Increasing beam diameter, leads to massive increase in melt-pool dimensions. The effect of preheating temperature on the melt-pool dimensions is also remarkable, however, melt-pool dimensions seems to be less sensitive to porosity in comparison with other factors.

As for melt-pool maximum temperature, Fig.21 is presenting the recording data:

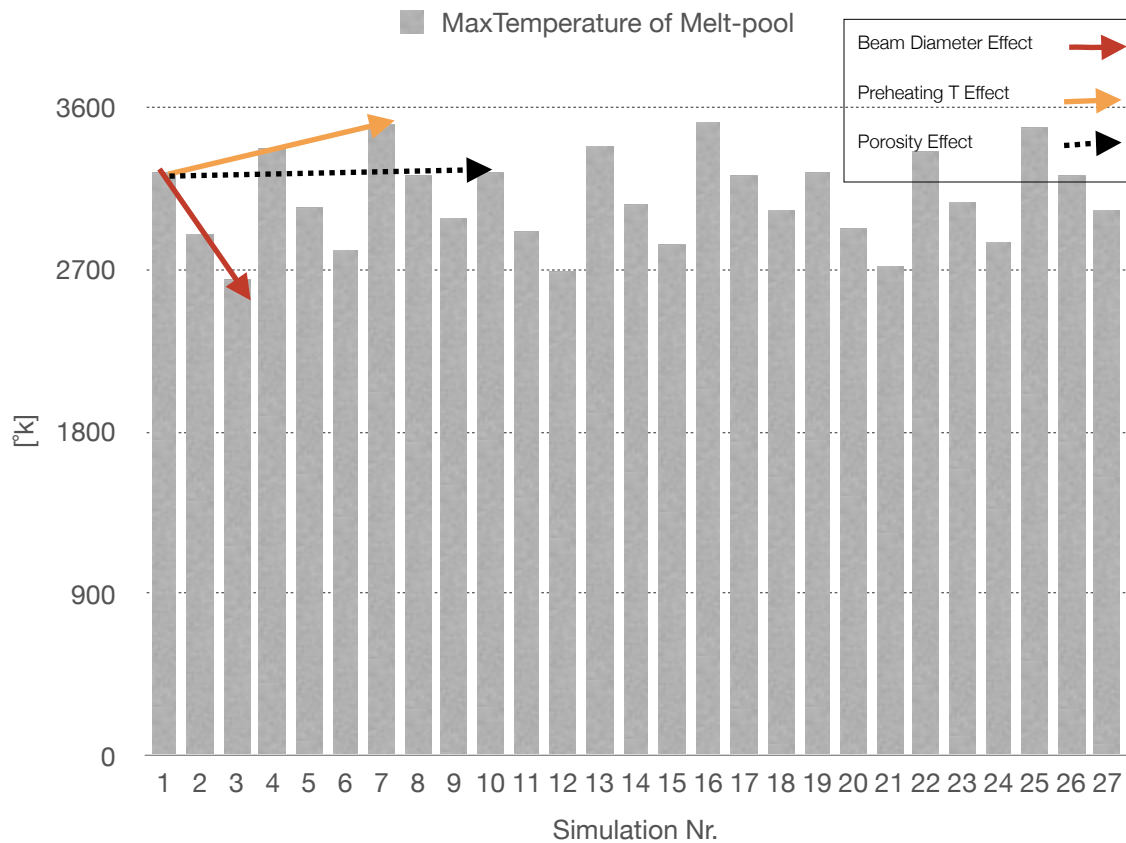


Fig.21: Melt-pool maximum temperature sensitivity to porosity, preheating temperature and beam diameter

As indicated in Fig.21, by increasing the preheating temperature, the maximum temperature of the melt-pool would be increased, on the other hand, the porosity factor seems to have slight effect on the melt-pool maximum temperature.

Regarding the beam diameter, this factor has significant effect on the melt-pool maximum temperature however, the maximum temperature will decrease by increasing the beam diameter.

Beside these general points, it is important to be more specific and investigate more details in order to obtain more accurate conclusion.

Melt-pool consist of 3 different dimensions, here we considered the effect of each parameter on each dimension separately:

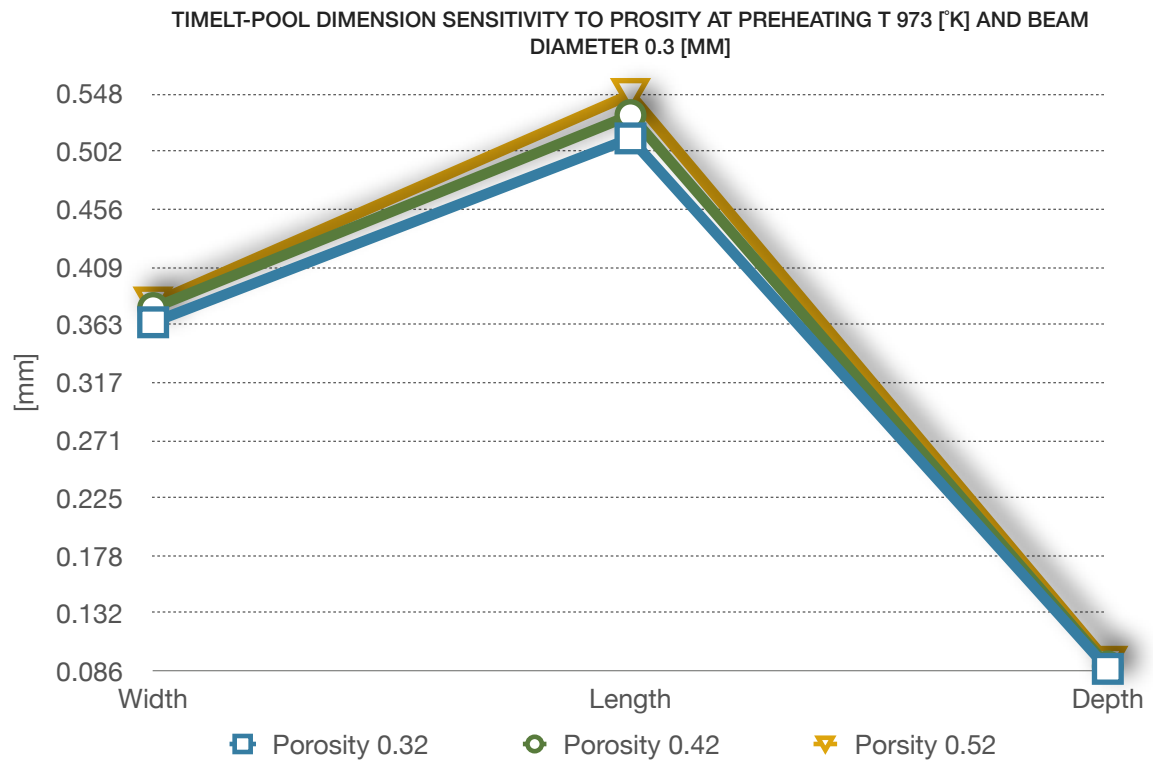


Fig.22: Porosity effect on melt-pool dimensions

In Fig.22 the effect of different porosities on the melt-pool dimensions has been demonstrated.

Based on the results of the simulations, the porosity has slight effect on the width and depth of the melt-pool, the length of the melt-pool seems to be more sensitive to porosity than other dimensional factors.

As for Fig.23 it can be seen, length of the melt-pool is enormously sensitive to preheating temperature than other dimensional characteristic. Moreover, by comparing Fig22, with Fig. 23, it is obvious that preheating temperature has a higher effect on melt-pool size in comparison to porosity parameter.

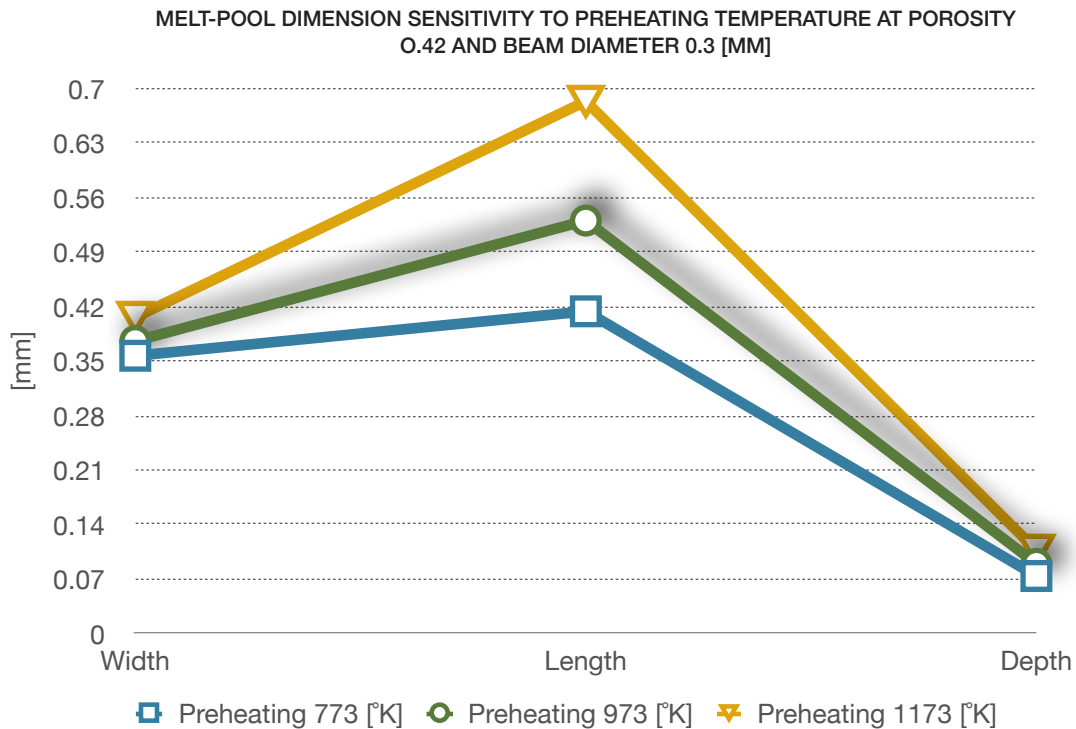


Fig.23: Preheating temperature effect on melt-pool dimensions

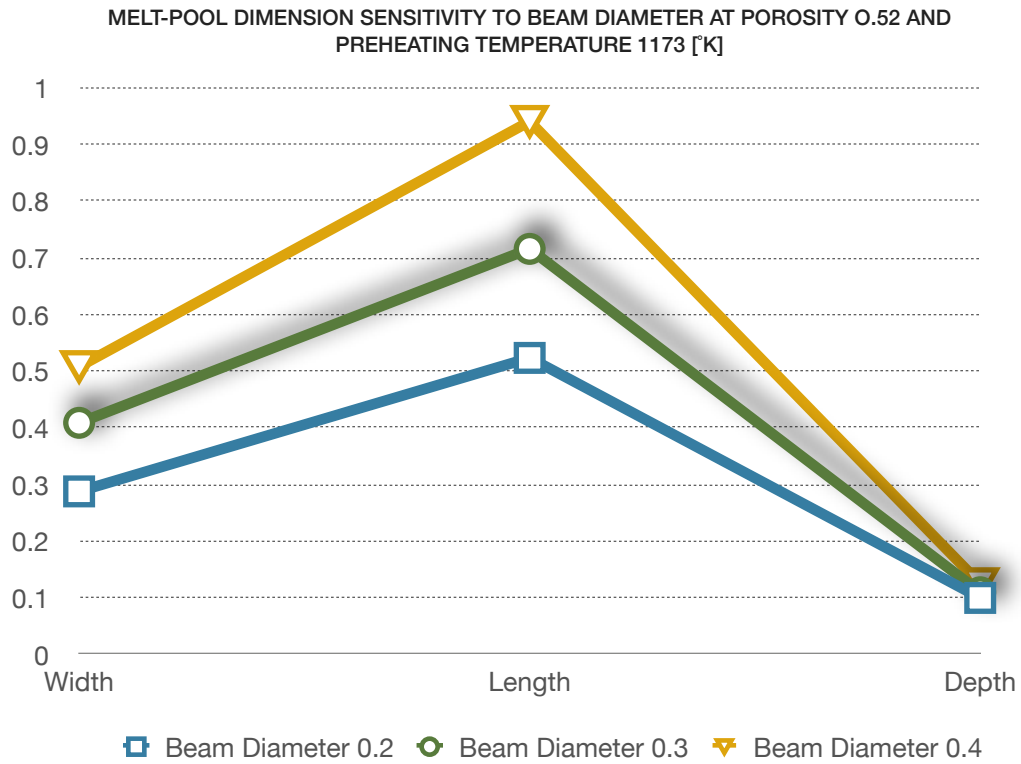


Fig.24: Beam diameter effect on melt-pool dimensions

Considering the last factor “beam diameter” Fig.24, the melt-pool length significantly is sensitive to the beam diameter, and width of the melt-pool is affected by beam diameter remarkably, although the depth factor seems to be less sensitive to this parameter.

Now, here in below, the effect of each factor on the maximum melt-pool temperature has been demonstrated:

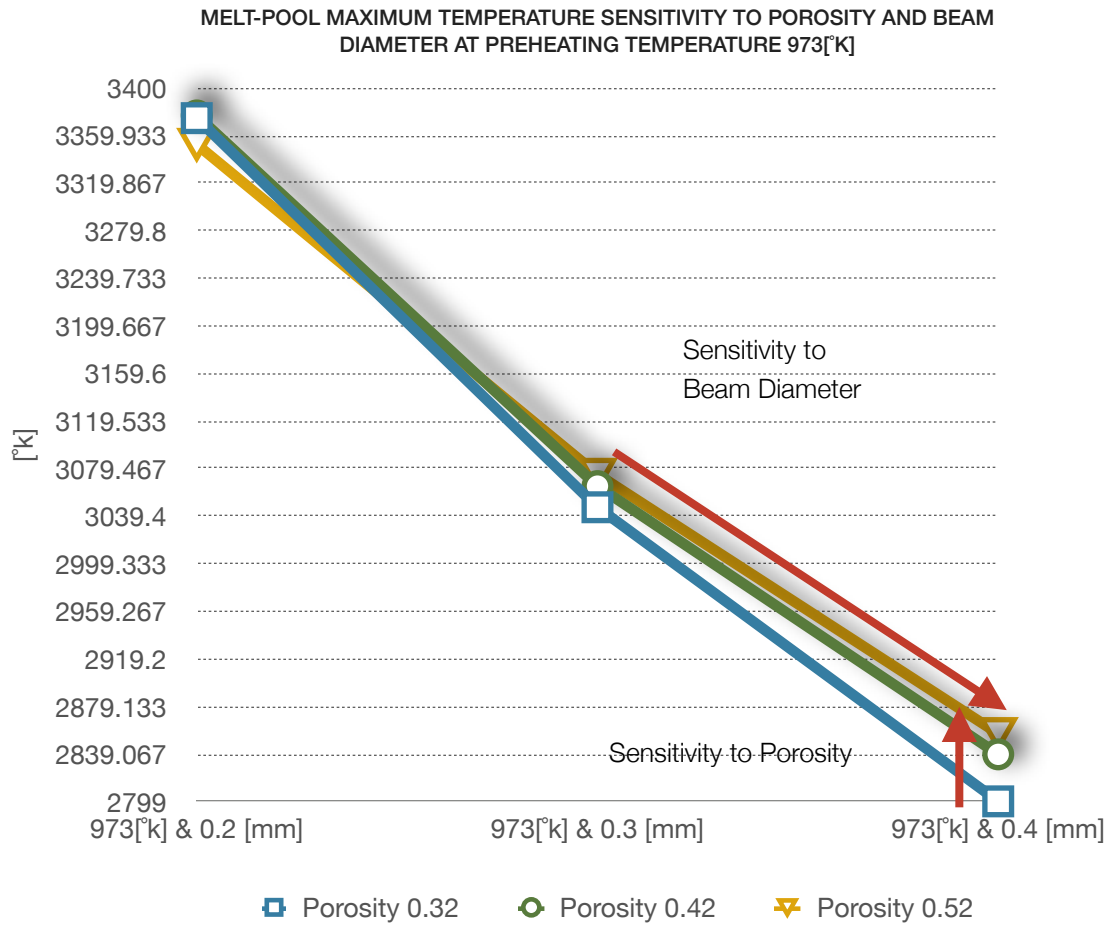


Fig.25: Porosity and Beam Diameter effects on the melt-pool maximum temperature

In the Fig.25 the effect of beam diameter has been compared with porosity at the preheating temperature 973°k.

As indicated in the figure, the melt-pool temperature has higher sensitivity to beam diameter in comparison powder porosity.

Moreover, it is noticeable that the effect of porosity at higher beam diameter (lower thermal flux) on the melt-pool temperature, is higher than that of the lower beam diameter.

Consequently, the melt-pool temperature shown to has a higher sensitivity to powder with lower porosity (higher density) than the powder with higher porosity (lower density).

In order to do an accurate comparison between beam diameter and preheating temperature, Fig.26 has been presented.

Beam diameter and preheating temperature are two parameters with higher effect on the melt-pool characteristics, therefore here we tried to point out their main features.

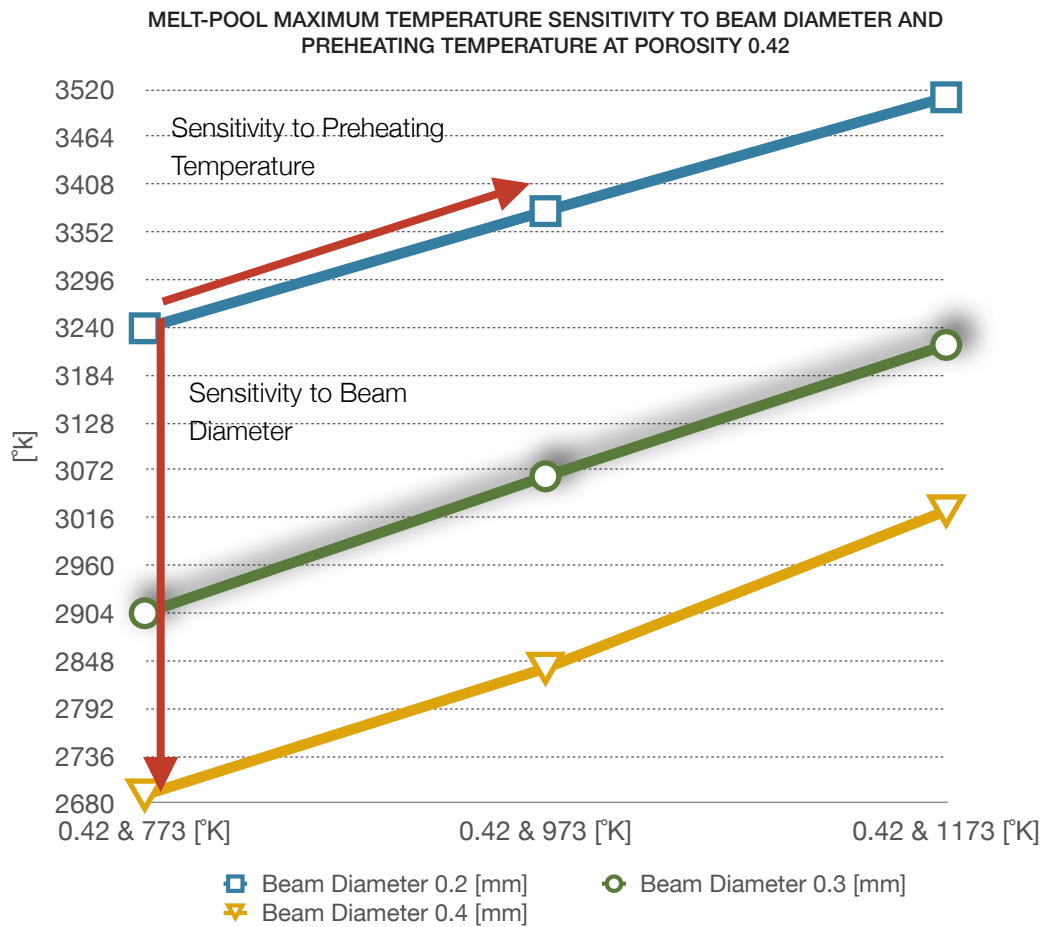


Fig.26: Preheating temperature and Beam Diameter effects on the melt-pool maximum temperature

In the Fig.26, the level of sensitivity of the melt-pool temperature to beam diameter and preheating temperature is been investigated clearly. The beam diameter has a higher effect, however the effect of preheating temperature is also remarkable.

On the other hand, the melt-pool maximum temperature characteristic has inverse relation with the beam diameter, unlike other parameter which have direct relation with the melt-pool maximum temperature. In this regard, table 12 has presented the heat flux correspond to each beam diameter.

In the table (13), all the results have been represented in order to have an overview.

Beam Diameter [mm]	Heat flux [w/mm2]
0.2	1256.1517
0.3	837.9771
0.4	611.5220

Table (12): Heat flux related to each beam diameter

Simulation Nr.	Porosity	T preheating	Beam diameter	Width	Length	Depth	Melt-pool Tmax
1	0.32	773	0.2	0.2554	0.3292	0.0707	3228.15
2	0.32	773	0.3	0.3526	0.4106	0.0734	2895.95
3	0.32	773	0.4	0.4166	0.4595	0.0702	2641.75
4	0.32	973	0.2	0.2698	0.3733	0.0833	3374.45
5	0.32	973	0.3	0.365	0.5121	0.0878	3046.99
6	0.32	973	0.4	0.4686	0.6178	0.0892	2799.48
7	0.32	1173	0.2	0.2826	0.5255	0.1011	3504.93
8	0.32	1173	0.3	0.375	0.6882	0.1073	3213.14
9	0.32	1173	0.4	0.492	0.8675	0.115	2990.48
10	0.42	773	0.2	0.276	0.3401	0.0705	3238.91
11	0.42	773	0.3	0.3568	0.4141	0.0735	2903.76
12	0.42	773	0.4	0.418	0.4907	0.0763	2690.02
13	0.42	973	0.2	0.2838	0.3735	0.082	3376.73
14	0.42	973	0.3	0.3764	0.5307	0.0897	3064.78
15	0.42	973	0.4	0.4638	0.6277	0.093	2839.04
16	0.42	1173	0.2	0.2918	0.5176	0.1014	3510.61
17	0.42	1173	0.3	0.4064	0.6842	0.1071	3219.32
18	0.42	1173	0.4	0.4758	0.8979	0.1208	3024.21
19	0.52	773	0.2	0.2752	0.3611	0.073	3231.09
20	0.52	773	0.3	0.3592	0.4114	0.075	2922.79
21	0.52	773	0.4	0.436	0.4916	0.0819	2714.31
22	0.52	973	0.2	0.2922	0.367	0.082	3352.38
23	0.52	973	0.3	0.3804	0.5472	0.093	3074.71
24	0.52	973	0.4	0.4686	0.6562	0.0979	2856.52
25	0.52	1173	0.2	0.288	0.5236	0.1	3486.27
26	0.52	1173	0.3	0.409	0.716	0.11	3221.04
27	0.52	1173	0.4	0.5082	0.9409	0.125	3033.87

Table (13): Sensitivity Analysis simulation results

CONCLUSION

Perspective and Objectives

Producing a part has always been dealt with time and material consumption. EBM technology has suggested low material consumption with high efficiency, however it needs some amount of time to produce a component. Although there has been lots of studies in order to reduce the time consumption in this technology, but it still has long way to go.

The overall objective of the present work is to define process parameters in a way that the foregoing deficiencies will be avoided and sample parts are able to be built faster and better. To do this, In this thesis we tried by applying some modifications in the material properties and process parameters through various simulation, obtain an optimum mode and consequently, reduce the time required to produce a part. Concerning this issue, melt pool characteristic play an important role.

As it has been explained in the pervious chapters, the parameters such as Powder Porosity, Preheating Temperature and Beam Diameter have been focused on in this thesis work and the simulation model has been run to understand the sensitivity of the melt-pool characteristic to aforementioned parameters. Based on the results that has been presented previously, here we want to highlight its features and its consequences:

In general point of view, as far as the melt-pool dimension is concerned, the sensitivity analysis suggest that the beam diameter has highest rate of effectivity to the melt-pool dimension among the other two parameters, although the effect of preheating temperature is significant as well.

On the other hand, the powder porosity shows less effect on the melt-pool dimension. Increasing the powder porosity (decreasing the powder density) leads to slight increase in the melt-pool dimensions.

More specifically, as shown in the Fig.22, among all the dimensional sectors, the effect of porosity seem to be higher on the “length” of the melt-pool than the other sectors. However the length of the melt-pool proofed to be more sensitive to preheating temperature and beam diameter as well. Unlike the “Length” it has been observed that the the depth of the melt-pool is not so sensitive to the parameters we have been considering.

Concerning the melt-pool maximum temperature, in general point of view, it can be seen by increasing the preheating temperature, the maximum temperature of the melt-pool increases, also by increasing the beam diameter, the maximum temperature of the melt-pool decreases significantly.

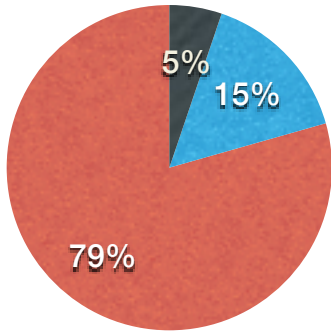
However, here we can see, by increasing the the porosity 0.32 to porosity 0.42 with same preheating temperature and same beam diameter, we observe a little increase in the melt-pool maximum temperature, which means it is no so sensitive to porosity. As a matter of fact, the increasing in porosity (decreasing in the powder density) leads to decrease in the thermal conductivity and consequently less heat transfer would occur and less increase would be appear on the melt-pool, in this regard as it can be seen in Fig.25, for the powder with higher density (lower porosity), increasing the thermal flux leads to higher maximum temperature at the melt-pool than the powder with lower density. which is also due to thermal conductivity.

Concerning the Beam diameter it is noticeable that this factor has different attitude regarding melt-pool maximum temperature and melt-pool dimensions, however in both cases, its effect is significant. Increasing in the beam diameter leads to increase in the melt-pool dimensions (mostly length and width) which is due to widening the spot size which consequently increase the dimensions of the melt-pool, on the other hand, since the increasing the beam diameter decreases the heat flux (Table 12), this matter leads to a remarkable decrease in the melt-pool maximum temperature.

Here in pie charts Fig.27, the sensitivity analysis is been classified in order to give better overview. As it is indicated in Fig.27, melt-pool width at higher heat fluxes (lower beam diameter) is more sensitive to porosity than the case with higher heat flux as for thermal conductivity effect.

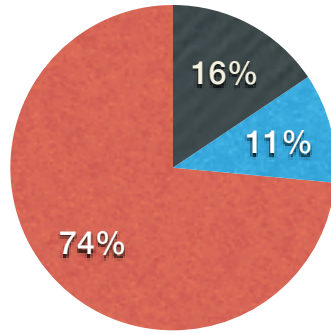
Regarding the melt-pool dimension, as it has been demonstrated in Fig.27, depth factor has lowest sensitivity to the parameter that has been studied in this thesis work, unlike the length sensitivity which is proofed to be significant to mentioned factors.

MELT-POOL WIDTH SENSITIVITY
COMPERISON AT 0.32_0.42 AND 773 _973
°K AND 0.3_0.4 MM



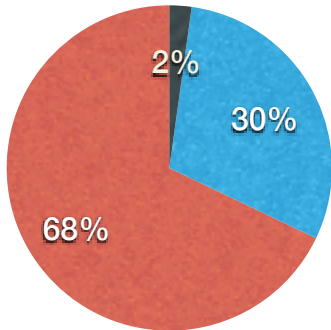
- Porsity Effect
- Preheating Temperature Effect
- Beam Diameter Effect

MELT-POOL WIDTH SENSITIVITY
COMPERISON AT 0.32-0.42 AND 773 _973
°K AND 0.2_0.3 MM



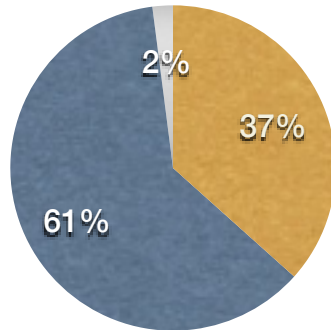
- Porsity Effect
- Preheating Temperature Effect
- Beam Diameter Effect

MELT-POOL MAXIMUM TEMPERATURE
SENSITIVITY



- Porsity Effect
- Preheating Temperature Effect
- Beam Diameter Effect

MELTPOOL DIMENSIONAL SENSITIVITY FO
BEAM DIAMETER



- Width Sensitivity
- Length Sensitivity
- Depth Sensitivity

Fig.27: Melt-pool characteristic sensitivity percentage to different parameters

Project Outline

After presenting the process parameter and material properties, 3 different factor “Preheating temperature”, “Powder porosity” and “Beam diameter” has been chosen for sensitivity analysis, and a plate sample model has been focused on in order to run the simulation. To cover all the possible effect of these factors the simulations have been run 27 times for each parameter modification.

Based on the results of the simulations, it is proofed that beam diameter has had highest effect on the melt-pool dimensions and and its maximum temperature. The effect of preheating temperature is also noticeable, however powder porosity has shown to have lower effect on the melt-pool characteristics.

Although the beam diameter has the highest effect, it might cause higher energy consumption to produce a part which is not sufficient in economic point of view. Therefore among the factors that has been studied in this thesis, the “Preheating temperature” seems to be more efficient considering both the production time and economic point of view. But then again, increasing the melt-pool dimension through beam diameter leads to decrease the melt-pool maximum temperature, therefore an reasonable balance between the these to factors could be an efficient solution in order to fix the beam diameter for production process.

BIBLIOGRAPHY

1. Soylemez E, Beuth JL, Taming K, editors. Controlling melt pool dimensions over a wide range of material deposition rates in electron beam additive manufacturing. Proceedings of 21st Solid Freeform Fabrication Symposium, Austin, TX, Aug; 2010.
2. Lutzmann S, Kahnert M, Sigl M. Elektronenstrahlsintern als Zukunftstechnologie im Rapid Tooling. Rapid Manufacturing: Heutige Trends-Zukünftige Anwendungsfelder. 2006;7-1.
3. Taming K, Hafley RA, Dicus DL. Solid freeform fabrication: an enabling technology for future space missions. 2002.
4. Davé VR. Electron beam (EB)-assisted materials fabrication: Massachusetts Institute of Technology; 1995.
5. Murr L, Quinones S, Gaytan S, Lopez M, Rodela A, Martinez E, et al. Microstructure and mechanical behavior of Ti-6Al-4V produced by rapid-layer manufacturing, for biomedical applications. Journal of the mechanical behavior of biomedical materials. 2009;2(1):20-32.
6. Safdar A, Wei L-Y, Snis A, Lai Z. Evaluation of microstructural development in electron beam melted Ti-6Al-4V. Materials Characterization. 2012;65:8-15.
7. Hrabe N, Quinn T. Effects of processing on microstructure and mechanical properties of a titanium alloy (Ti-6Al-4V) fabricated using electron beam melting (EBM), Part 2: Energy input, orientation, and location. Materials Science and Engineering: A. 2013;573:271-7.
8. Wang P, Nai MLS, Sin WJ, Wei J, editors. Effect of building height on microstructure and mechanical properties of big-sized Ti-6Al-4V plate fabricated by electron beam melting. MATEC Web of Conferences; 2015: EDP Sciences.
9. Tan X, Kok Y, Tan YJ, Vastola G, Pei QX, Zhang G, et al. An experimental and simulation study on build thickness dependent microstructure for electron beam melted Ti-6Al-4V. Journal of Alloys and Compounds. 2015;646:303-9.
10. Wang P, Tan X, Nai MLS, Tor SB, Wei J. Spatial and geometrical-based characterization of microstructure and microhardness for an electron beam melted Ti-6Al-4V component. Materials & Design. 2016;95:287-95.
11. Jamshidinia M, Kong F, Kovacevic R. Numerical modeling of heat distribution in the electron beam melting® of Ti-6Al-4V. Journal of Manufacturing Science and Engineering. 2013;135(6):061010.

12. Raghavan S, Nai MLS, Wang P, Sin WJ, Li T, Wei J. Heat treatment of electron beam melted (EBM) Ti-6Al-4V: microstructure to mechanical property correlations. *Rapid Prototyping Journal*. 2018;24(4):774-83.
13. DeCarlo RA, Mathur AP. Using sensitivity analysis to validate a state variable model of the software test process. *IEEE Transactions on Software Engineering*. 2003(5):430-43.
14. Kozak J, Zakrzewski T, editors. Accuracy problems of additive manufacturing using SLS/SLM processes. *AIP Conference Proceedings*; 2018: AIP Publishing.
15. Mirkoohi E, Ning J, Bocchini P, Fergani O, Chiang K-N, Liang S. Thermal modeling of temperature distribution in metal additive manufacturing considering effects of build layers, latent heat, and temperature-sensitivity of material properties. *Journal of Manufacturing and Materials Processing*. 2018;2(3):63.
16. Criaes LE, Arsoy YM, Özel T. Sensitivity analysis of material and process parameters in finite element modeling of selective laser melting of Inconel 625. *The International Journal of Advanced Manufacturing Technology*. 2016;86(9-12):2653-66.
17. Roberts IA, Wang C, Esterlein R, Stanford M, Mynors D. A three-dimensional finite element analysis of the temperature field during laser melting of metal powders in additive layer manufacturing. *International Journal of Machine Tools and Manufacture*. 2009;49(12-13):916-23.
18. Conti P, Cianetti F, Pileri P. Parametric Finite Elements Model of SLM Additive Manufacturing process. *Procedia Structural Integrity*. 2018;8:410-21.
19. Galati M, Iuliano L. A literature review of powder-based electron beam melting focusing on numerical simulations. *Additive Manufacturing*. 2017.
20. Galati M, Iuliano L, Salmi A, Atzeni E. Modelling energy source and powder properties for the development of a thermal FE model of the EBM additive manufacturing process. *Additive Manufacturing*. 2017;14:49-59.
21. Wang L, Felicelli SD, Craig JE. Experimental and numerical study of the LENS rapid fabrication process. *Journal of Manufacturing Science and Engineering*. 2009;131(4): 041019.
22. Galarraga H, Warren RJ, Lados DA, Dehoff RR, Kirka MM, Nandwana P. Effects of heat treatments on microstructure and properties of Ti-6Al-4V ELI alloy fabricated by electron beam melting (EBM). *Materials Science and Engineering: A*. 2017;685:417-28.
23. Karayagiz K, Elwany A, Tapia G, Franco B, Johnson L, Ma J, et al. Numerical and Experimental Analysis of Heat Distribution in the Laser Powder Bed Fusion of Ti-6 Al-4 V. *IJSE Transactions*. 2018(just-accepted):1-44.
24. Madenci E, Guven I. The finite element method and applications in engineering using ANSYS®: Springer; 2015.

25. Ladani L, Romano J, Brindley W, Burlatsky S. Effective liquid conductivity for improved simulation of thermal transport in laser beam melting powder bed technology. *Additive Manufacturing*. 2017;14:13-23.
26. Foroozmehr A, Badrossamay M, Foroozmehr E. Finite element simulation of selective laser melting process considering optical penetration depth of laser in powder bed. *Materials & Design*. 2016;89:255-63.
27. Parthasarathy J, Starly B, Raman S, Christensen A. Mechanical evaluation of porous titanium (Ti6Al4V) structures with electron beam melting (EBM). *Journal of the mechanical behavior of biomedical materials*. 2010;3(3):249-59.
28. Neikter M, Forsberg F, Pederson R, Antti M-L, Åkerfeldt P, Larsson S, et al. Defect characterization of electron beam melted Ti-6Al-4V and Alloy 718 with X-ray microtomography. *Aeronautics and Aerospace Open Access Journal*. 2018;2(3):139-45.